Published in final edited form as:

Nat Neurosci. 2017 December ; 20(12): 1752–1760. doi:10.1038/s41593-017-0010-3.

Social stress induces neurovascular pathology promoting depression

Caroline Menard[1,8], **Madeline L. Pfau**[1], **Georgia E. Hodes**[1], **Veronika Kana**[2], **Victoria X. Wang**[3], **Sylvain Bouchard**[1], **Aki Takahashi**[1,4], **Meghan E. Flanigan**[1], **Hossein Aleyasin**[1], **Katherine B. LeClair**[1], **William G. Janssen**[1], **Benoit Labonté**[1], **Eric M. Parise**[1], **Zachary S. Lorsch**[1], **Sam A. Golden**[1], **Mitra Heshmati**[1], **Carol Tamminga**[5], **Gustavo Turecki**[6], **Matthew Campbell**[7], **Zahi Fayad**[3], **Cheuk Ying Tang**[3], **Miriam Merad**[2], and **Scott J. Russo**[1,*]

[1]Fishberg Department of Neuroscience and the Friedman Brain Institute, Icahn School of Medicine at Mount Sinai [2]Department of Oncological Science, Tisch Cancer Institute and Immunology Institute, Icahn School of Medicine at Mount Sinai [3]Departement of Radiology, Translational and Molecular Imaging Institute at Mount Sinai, New York, USA [4]University of Tsukuba, Japan [5]Department of Psychiatry, the University of Texas Southwestern Medical Center, USA [6]Douglas Mental Health University Institute and McGill University, Canada [7]Trinity College, Dublin, Ireland

Abstract

Studies suggest that heightened peripheral inflammation contributes to the pathogenesis of major depressive disorder. We investigated the effect of chronic social defeat stress, a mouse model of depression, on blood-brain barrier (BBB) permeability and infiltration of peripheral immune signals. We found reduced expression of endothelial cell tight junction protein claudin-5 (cldn5) and abnormal blood vessel morphology in nucleus accumbens (NAc) of stress-susceptible but not resilient mice. *CLDN5* expression was also decreased in NAc of depressed patients. *Cldn5* down-regulation was sufficient to induce depression-like behaviors following subthreshold social stress while chronic antidepressant treatment rescued cldn5 loss and promoted resilience. Reduced BBB integrity in NAc of stress-susceptible or AAV-shRNA-*cldn5*-injected mice caused infiltration of peripheral cytokine interleukin-6 (IL-6) into brain parenchyma and subsequent expression of

[*]**Corresponding author**: Scott J. Russo, scott.russo@mssm.edu.

[8]**Present address:** Département de psychiatrie et neurosciences, Faculté de médecine and CERVO Brain Research Center, Université Laval, Quebec City, Canada

Author Contributions

C.M. and S.J.R. designed the study and wrote the manuscript. C.M., M.L.P., G.E.H., A.T., M.E.F., H.A., K.B.L., Z.S.L., S.A.G. and M.H. performed stereotaxic surgeries, tissue collection, behavioral manipulations and analyzed data. V.K. performed and analyzed flow experiments and ccr2^{RFP}/cx3cr1^{GFP} immunostaining, V.K. and M.M. provided *ccr2*^{RFP}:: *cx3cr1*^{GFP} mice and provided advise on BBB- and immune-related studies. V.X.W., Z.F. and C.Y.T. designed, performed and analyzed magnetic resonance imaging scans. S.B. advised on analysis approaches and analyzed data, W.G.J. prepared and imaged transmission electron microscopy samples. B.L., E.M.P., C.T. and G.T. provided postmortem human tissue samples. M.C. provided viral vectors and advised on viral studies. All the authors read and commented on the manuscript.

Competing financial interests

The authors wish to declare no competing financial interest.

depression-like behaviors. These findings suggest that chronic social stress alters BBB integrity through loss of tight junction protein cldn5, promoting peripheral IL-6 passage across the BBB and depression.

Introduction

Major depressive disorder (MDD) is the leading cause of worldwide disability and the most prevalent mood disorder[1, 2]. The prevalence of MDD is two to three-fold higher in patients suffering from cardiovascular disease and conversely, MDD is associated with an ~80% increased risk of cardiovascular morbidity and mortality[1, 3–5]. Chronic inflammation and sustained increases in circulating pro-inflammatory cytokines have been associated with atherosclerotic plaque formation, progression, and rupture, likely contributing to the pathogenesis of cardiovascular disease and heart failure [6]. Concomitantly, clinical studies report higher levels of circulating pro-inflammatory cytokines in MDD patients, a pattern that has been replicated in preclinical animal models of depression[1, 7–10]. Individual differences in the peripheral immune system and modulation of cytokine release, notably interleukin-6 (IL-6), are associated with susceptibility versus resilience to chronic social stress[11]. Chronic stress mobilizes the innate immune system and stimulates enhanced proliferation and release of inflammatory monocytes and neutrophils into the bloodstream[12, 13].

It has been hypothesized that peripheral myeloid cells or pro-inflammatory cytokines can diffuse into the brain of stressed individuals due to stress-induced neurovascular damage and increased blood-brain barrier (BBB) permeability[7, 14–19]. Indeed, a clinical study reported altered cerebrospinal fluid to serum ratio of peripheral markers in depressed patients, suggesting that BBB integrity is compromised[20]. However, the possible link between BBB permeability, stress vulnerability and depression is still controversial[21]. The BBB is formed by endothelial cells sealed by tight junction proteins, pericytes and astrocytes, and serves to prevent potentially harmful signals in the blood from entering the brain. Here, we evaluated the effect of chronic social defeat stress (CSDS), a mouse model of depression, on BBB-related gene expression and define a role for the tight junction protein claudin 5 (Cldn5) in the establishment of depression-like behaviors and MDD. Cldn5 is a major cell adhesion molecule of endothelial cells[22] and loss of Cldn5 has been shown to promote loosening of the BBB and increased permeability[23]. Our study is the first to characterize and functionally interrogate the neurovascular pathology associated with social stress vulnerability.

Results

Vulnerability to chronic social stress and MDD are associated with loss of tight junction protein cldn5 expression

Chronic social stress is a prominent contributor to mood disorder prevalence and suicide attempts in victims of bullying[24]. Similarly, in rodents, CSDS induces a depression-like phenotype (social avoidance, anhedonia) in a subset of mice termed stress-susceptible (SS) that can be reversed only by chronic, but not acute, antidepressant treatment[25, 26]. In the CSDS protocol, male C57BL/6J mice are exposed daily (10 min/day) to bouts of social

defeat by a larger, physically aggressive CD-1 mouse[27] (Fig. 1A). Defeated mice that do not display social avoidance as assessed with the social interaction (SI) test (Supplementary Fig. 1A–C) are considered resilient (RES). We compared SS to RES mice to identify individual differences in the neurovascular mechanisms potentially underlying chronic stress responses. First, we performed transcriptional profiling of BBB-related and cytokine/chemokine gene expression in the nucleus accumbens (NAc) of unstressed control (CTRL), SS and RES mice after 10-day CSDS (Fig. 1B, qPCR primers are listed in Supplementary Information Table 1). The NAc plays a crucial role in stress responses and mood disorders including MDD[28]. CSDS induced changes in the expression of genes involved in endothelial cell biology, angiogenesis, vascular permeability, and BBB formation and function (Fig. 1B). Interestingly, *cldn5* mRNA was significantly reduced in NAc of SS mice compared to CTRL and RES mice and levels positively correlated with social avoidance behavior (**$p = 0.0014$) (Fig. 1C–E). Normalization of *cldn5* and other tight junction mRNA expression to platelet endothelial cell adhesion molecule (*pecam1*), an endothelial cell marker also known as cluster of differentiation 31 (CD31), confirmed ~40% loss of *cldn5* expression in SS mice (***$p = 0.0009$) (Supplementary Fig. 1D, E). Cldn5 is an endothelial cell-specific tight junction protein (Supplementary Fig. 2D)[29, 30], which we confirmed to be enriched in blood vessels using a brain capillary extraction method (Supplementary Fig. 2E). We next report a specific reduction of cldn5 protein in SS mice by examining its co-localization with CD31 (Fig. 1F). Cldn5 protein levels in NAc blood vessels also positively correlated with social avoidance behavior (**$p = 0.0014$) (Fig. 1G and Supplementary Fig. 2A–C). No difference was observed for CD31 or other tight junction proteins in the NAc (Supplementary Fig. 2F).

We next evaluated whether significant changes in *cldn5* expression were present after CSDS in other brain regions that contribute to depression symptomatology[28]. *Cldn5* mRNA levels in the hippocampus (HIPP) of both SS and RES mice were significantly lower than in unstressed CTRL mice (**$p = 0.0024$) (Supplementary Fig. 1F). However, cldn5 and occludin protein levels were significantly higher in the HIPP of RES mice when compared to SS mice but not controls, suggesting compensatory mechanisms in this brain region (Supplementary Fig. 3A). No difference was observed between SS, RES, and CTRL mice in the prefrontal cortex (PFC) or hypothalamus (Supplementary Fig. 1G–H, 3B). We next used transmission electron microscopy to show that CSDS induces ultrastructural abnormalities of blood vessels within the NAc of SS, but not RES, mice (Fig. 1I, Supplementary Fig. 4A–C). In SS mice, blood vessels were characterized by discontinuous tight junctions (***$p < 0.0001$) (Fig. 1I). Ultrastructural abnormalities were present in both large vessels and capillaries of the NAc (Supplementary Fig. 4D). No significant change was observed in the PFC of SS or RES mice when compared to unstressed CTRL mice (Supplementary Fig. 4E).

Additionally, we evaluated the effect of non-social chronic stressors on *cldn5* expression in the NAc. Male C57BL/6J mice subjected to 28 days of chronic variable stress (CVS), which also induces a depression-like phenotype, displayed reduced *cldn5* mRNA expression in the NAc (**$p = 0.0089$) (Supplementary Fig. 1J). However, no change was observed after six days of variable stress (subchronic variable stress or SCVS), a protocol that is insufficient to induce depression-like behaviors in male mice[31] (Supplementary Fig. 1I). These findings suggest that stress-induced reduction of *cldn5* expression occurs in multiple brain regions in response to both social and non-social stress; however, cldn5 downregulation by stress does

not occur ubiquitously throughout the brain and therefore likely plays a specialized role in depression-like symptomatology.

Chronic antidepressant treatment can reverse CSDS-induced depression-like behaviors, including social avoidance[25, 32]. Thus, we evaluated the effect of chronic imipramine treatment on *cldn5* expression in the NAc of SS mice. Following CSDS and behavioral phenotyping by SI, SS mice were treated with either vehicle or imipramine via i.p. injection (20 mg/kg of body weight) for 35 days alongside unstressed vehicle or imipramine control groups (Supplementary Fig. 5A). As expected, social avoidance was rescued in the imipramine-treated, but not vehicle-treated, group (interaction treatment x stress: $*p = 0.0201$) (Fig. 1H and Supplementary Fig. 5B–D). Chronic imipramine treatment also normalized *cldn5* mRNA expression in the NAc of SS mice (Fig. 1H), while acute imipramine injection was not sufficient to alter *cldn5* mRNA (Supplementary Fig. 5E) or social avoidance[32]. Finally, we evaluated *CLDN5* mRNA expression in postmortem NAc tissue from subjects with MDD. We used samples from two independently collected MDD cohorts, one from McGill University (Montreal cohort) and a second from the University of Texas Southwestern Medical Center (Texas cohort). About half of the MDD subjects in each cohort were on medication at time of death as determined by toxicology reports (Supplementary Information Table 2–3). *CLDN5* mRNA expression was significantly reduced in the NAc of non-medicated MDD patients when compared to healthy controls in the Montreal cohort ($*p = 0.0117$) and this effect was only partially rescued by medication (Fig. 1J and Supplementary Fig. 5F). In the Texas cohort, *CLDN5* mRNA level was significantly reduced between MDD patients and healthy controls ($*p = 0.0435$) with no effect of medication (Fig. 1J and Supplementary Fig. 5F). No significant difference was observed for HIPP and PFC when compared to healthy subjects (Supplementary Fig. 5G). Lack of significant medication effects may be related to suicide as cause of death for the majority of MDD patients in our cohorts. In addition, loss of *CLDN5* may be at least partly specific to mood disorders as no change was observed in postmortem NAc tissue from cocaine users when compared to healthy controls (Supplementary Fig. 5H).

Downregulation of cldn5 expression induces depression-like behaviors

To confirm a causal role for cldn5 downregulation in social stress-induced depression-like behaviors, we conducted functional studies using viral-mediated, conditional knockdown of cldn5 in the NAc. We chose this conditional approach because cldn5-deficient mice die within 10 h of birth[23] and social stress was performed in adult mice. Stress-naïve adult male mice received stereotactic, intra-NAc injections of adeno-associated virus (AAV-2/9 serotype) expressing a doxycycline-inducible, *cldn5*-targeting shRNA transcript (AAV-shRNA-*cldn5*) or a control non-targeting vector (AAV-shRNA)[33]. We confirmed that injection of AAV-shRNA-*cldn5* virus into the NAc followed by treatment with doxycycline induces downregulation of *cldn5* mRNA ($**p = 0.0016$) (Fig. 2B) and protein ($**p = 0.0013$) (Fig. 2C) levels. No change was observed for other claudins or markers of endothelial cells, pericytes, astrocytes and microglia (Supplementary Fig. 6A, qPCR primers are listed in Supplementary Information Table 4) or protein level of endothelial cell marker CD31 (Supplementary Fig. 6B). For behavioral studies, mice were again injected with AAV-shRNA-*cldn5* or AAV-shRNA, and then allowed two weeks recovery, prior to doxycycline

treatment to induce expression of *cldn5*-shRNA. Half of the mice were subjected to a subthreshold micro-defeat consisting of three 5-min bouts of social defeat, each separated by a 15-min period of rest (Fig. 2A). Without the introduction of pro-depressive manipulations, this protocol is insufficient to induce depression-like behaviors and thus can be used to identify pro-susceptibility factors[32]. All AAV-injected mice were then subjected to a battery of depression- and anxiety-related behavioral tests (Fig. 2A). Loss of cldn5 did not affect baseline depression-like behaviors; however, when combined with subthreshold micro-defeat, *cldn5* downregulation induced depression-like behaviors across multiple behavioral assays. Stressed AAV-shRNA-*cldn5* mice spent significantly less time grooming in the splash test (*$p = 0.0356$) (Fig. 2D), displayed anhedonia as assessed with the sucrose preference test (**$p = 0.0063$) (Fig. 2E), and spent more time immobile in the forced swim test (**$p = 0.0015$) (Fig. 2F). They also displayed greater social avoidance when compared to unstressed controls and stressed AAV-shRNA mice as measured by lower social interaction ratio (*$p = 0.0386$) (Fig. 2G), less time spent in the interaction zone (**$p = 0.0064$), and more time spent in the corners (*$p = 0.0463$) when the social target was present (Supplementary Fig. 6C). On the other hand, AAV-shRNA-*cldn5* had no effect on anxiety-related behaviors as assessed with the novelty-suppressed feeding (Supplementary Fig. 6D), elevated plus maze (Supplementary Fig. 6E) and open field (Supplementary Fig. 6F). Because we observed higher cldn5 protein level in RES mice after 10-day CSDS when compared to SS mice (Supplementary Fig. 3A), we also evaluated the effect of viral-mediated down-regulation of *cldn5* expression in this brain region. Injection of AAV-sRNA-*cldn5* and AAV-shRNA viruses in the HIPP (Supplementary Fig. 7A–B) had no effect on grooming in the splash test or sucrose preference however stressed AAV-shRNA-*cldn5* mice displayed greater social avoidance (***$p = 0.0005$) (Supplementary Fig. 7C–F). Mice injected with AAV-shRNA-*cldn5* also spent more time immobile in the forced swim test (two-way ANOVA, virus effect: *$p = 0.0396$) (Supplementary Fig. 7E), suggesting a region-specific effect for some, but not all, behaviors. Finally, we performed a rescue experiment to confirm the causal role of NAc *cldn5* expression in the establishment of depression-like behaviors (Fig. 2H, Supplementary Fig. 7G). Two cohorts of mice were injected with either AAV-shRNA-*cldn5* or AAV-shRNA and allowed two weeks recovery, prior to doxycycline treatment to induce expression of *cldn5*-shRNA. Half of the mice in each cohort were subjected to a subthreshold micro-defeat and establishment of depression-like behaviors was confirmed in stressed AAV-shRNA-*cldn5* mice with forced swim test and sucrose preference test (Fig. 2H–I, Supplementary Fig. 7J). Afterwards, doxycycline treatment was stopped for one cohort of mice (Fig. 2H) allowing recovery of *cldn5* expression[33], which was confirmed at both mRNA and protein levels (Supplementary Fig. 7H). Recovery of normal cldn5 expression reversed anhedonia and promoted resilience in the social interaction test in stressed AAV-shRNA-*cldn5* mice (Fig. 2J). Conversely, stressed AAV-shRNA-*cldn5* mice in the second cohort remaining on doxycycline (Supplementary Fig. 7G) displayed anhedonia, social avoidance (Supplementary Fig. 7K) and lower cldn5 mRNA and protein levels (Supplementary Fig. 7I). These findings suggest that cldn5 expression plays a protective role in behavioral response to social stress, possibly by maintaining BBB impermeability to stress-induced passage of peripheral immune signals.

Chronic social stress alters blood vessel ultrastructure, promoting blood-brain barrier leakiness and passage of peripheral signals into the brain

Taking into account CSDS-induced loss of cldn5 and altered blood vessel morphology in SS mice, we next compared BBB integrity in CTRL, SS and RES mice following 10-day CSDS using a gadolinium-contrasting agent (Gd-DTPA, 0.7 kDa) and magnetic resonance imaging (MRI) scans (Fig. 3A and Supplementary Fig. 8A–C). Higher Gd-DTPA signal was detected in the NAc (*$p = 0.0237$) and HIPP (**$p = 0.0085$) of SS mice compared to CTRL and RES mice (Fig. 3B), suggesting leakiness of the BBB in these brain areas. Accordingly, injection of AAV-shRNA-*cldn5* enhances passive diffusion of Gd-DTPA from the blood into the brain[33], reinforcing the role of Cldn5 in maintaining BBB integrity under stressful conditions. Here we find that social avoidance was significantly correlated with Gd-DTPA level in the NAc (*$p = 0.0271$) (Fig. 3B–C, Supplementary Fig. 8D) and HIPP (*$p = 0.0335$) (Fig. 3B and Supplementary Fig. 8D–E) but not PFC (Supplementary Fig. 8F). We confirmed stress-induced BBB leakiness in the NAc (**$p = 0.0022$) (Fig. 3D–E) and HIPP of SS mice with cadaverine Alexa Fluor-555, a dye with a molecular weight of 0.95 kDa, which is similar to Gd-DTPA (Supplementary Fig. 8G–L). Again, accumulation of cadaverine Alexa Fluor-555 was significantly correlated with social avoidance (Supplementary Fig. 8J–K). Next, we examined infiltration of Evans blue (EB) dye following 10-day CSDS in stress-related brain regions. EB has a very high affinity for serum albumin (~69 kDa) (Fig. 3E, **left**), which cannot readily cross the BBB in the absence of neurovascular damage. We measured a significant infiltration of EB in the NAc of SS mice (**$p = 0.0014$) when compared to CTRL and RES groups (Fig. 3E), and EB level correlated with social avoidance behavior (**$p = 0.0018$) (Supplementary Fig. 9A–D). The dye seemed to accumulate in the perivascular space of NAc blood vessels but not within the brain parenchyma (Fig. 3E, right). Interestingly, no significant accumulation of EB was observed in the HIPP or PFC of defeated mice (Supplementary Fig. 9E–H), suggesting that the NAc BBB may be more vulnerable to neurovascular damage than that of other brain regions, leading to greater infiltration of larger proteins following stress. We confirmed BBB leakiness in the NAc of AAV-shRNA-*cldn5*-injected adult mice by injecting Alexa Fluor-555-conjugated cadaverine (two-way ANOVA virus effect: *$p = 0.0356$) and EB (two-way ANOVA virus effect: *$p < 0.0001$), an effect exacerbated by stress (two-way ANOVA stress effect: *$p = 0.0293$) (Fig. 3F–H). Finally, we compared the distribution of horseradish peroxidase (HRP, ~44 kDa) by transmission electron microscopy following 10-day CSDS. We found increased HRP uptake in the endothelium of SS mice (***$p = 0.0008$) (Fig. 3I). Together, these observations indicate that BBB integrity is impaired in SS, but not RES mice, in line with a loss of Cldn5 and abnormal blood vessel ultrastructure.

Previous studies report conflicting findings with regard to infiltration of peripheral immune cells into the brain following social stress[14, 34]. Considering the impact of 10-day CSDS on BBB permeability in the NAc of SS mice, we addressed this question by evaluating whether peripheral C-C chemokine receptor 2 (ccr2+) monocytes can infiltrate the brain parenchyma in stress-related brain regions. 10-day CSDS induced drastic changes in cytokine and chemokine mRNA expression in the NAc of defeated animals (Fig. 1B–C), including a significant increase of *ccr2* in SS mice (***$p < 0.0001$), which correlated with social avoidance (**$p = 0.0025$) (Supplementary Fig. 9I). We took advantage of *ccr2*^{RFP}::

cx3cr1^{GFP} double heterozygous mice [35] in which adult resident microglia exhibit a *ccr2*$^{RFP-}$/*cx3cr1*$^{GFP+}$ pattern[35, 36], whereas peripheral monocytes, which are recruited in response to inflammation, are characterized by a *ccr2*$^{RFP+}$/*cx3cr1*$^{GFP-}$ pattern[35–37]. *Ccr2*^{RFP}:: *cx3cr1*^{GFP} mice were subjected to 10-day CSDS, followed by a SI test. Half of the brain was collected for flow cytometry analyses and the other half fixed for immunohistochemistry (IHC) (Fig. 4A). As expected, stressed mice displayed social avoidance when compared to unstressed controls (*$p = 0.0103$) (Fig. 4B and Supplementary Fig. 9J). Flow cytometry revealed more *ccr2*$^{RFP+}$/*cx3cr1*$^{GFP-}$ peripheral monocytes in the brain of stressed bitransgenic mice compared to unstressed controls (*$p = 0.0479$) (Fig. 4C), with no change in *ccr2*$^{RFP-}$/*cx3cr1*$^{GFP+}$ resident microglia (Supplementary Fig. 9K, L). However, further analysis by IHC revealed that peripheral monocytes accumulate within ventricular space and NAc blood vessels, but do not infiltrate the brain parenchyma (Supplementary Fig. 9M).

Next, we evaluated whether circulating IL-6 (~21 kDa), a pro-inflammatory cytokine associated with stress vulnerability and MDD[7, 11], can infiltrate the NAc of defeated mice. We previously reported a 27-fold increase in circulating IL-6 level 20-min after defeat in SS mice[11]. No difference in basal IL-6 was observed before stress and IL-6 remained elevated in SS mice 48h after the last defeat[11]. Following 10-day CSDS (Supplementary Fig. 10A), we first confirmed higher IL-6 protein level in the blood of SS mice 48h after the last defeat (Fig. 4D). We also found higher IL-6 protein level in NAc compared to unstressed CTRL mice (*$p = 0.0321$) (Fig. 4D), although this does not rule out the possibility that stress induces local production of IL-6. No difference was observed for HIPP and PFC (Supplementary Fig. 10B), suggesting a region-specific accumulation of IL-6 in the NAc of SS mice following CSDS. To determine whether peripheral IL-6 is able to penetrate into the brain parenchyma of SS mice, we tagged mouse recombinant IL-6 with biotin (~0.45 kDa) and injected it retro-orbitally into the blood of CTRL, SS or RES mice (Fig. 4G and Supplementary Fig. 10D–G). Two hours later, animals were perfused and brains were collected and the expression of biotinalyted-IL6 in the brain was assessed using a NeutrAvidin Oregon-488 conjugated secondary antibody. Interestingly, biotinylated-IL6 was only detectable in the NAc of SS mice and labeling with the perivascular marker CD31 revealed passage outside of blood vessels into the parenchyma (Fig. 4G). Biotinylated-IL6 was undetectable in the HIPP or PFC of SS mice (Supplementary Fig. 10F–G). Importantly, our studies also revealed that the NAc is largely impermeable to circulating IL-6 under normal conditions as we were unable to detect biotinalyted-IL6 in the NAc of unstressed CTRL mice (Fig. 4G) and i.p. injections of recombinant IL-6 did not increase levels of IL-6 in NAc of naive mice (Fig. 4E) despite there being a large increase in the blood of these mice (Supplementary Fig. 10C). Importantly, downregulation of *cldn5* expression with an AAV-shRNA allows the passage of biotinylated-IL6 in the NAc parenchyma (Fig. 4H). To confirm the importance of NAc IL-6 in the establishment of depression-like behaviors, cannula were implanted in the NAc of stress-naïve mice and either saline or IL-6 was infused before subthreshold micro-defeat (Fig. 4F). Stressed mice that received intra-NAc IL-6 displayed social avoidance compared to stressed mice receiving intra-NAc saline or unstressed mice receiving either intra-NAc IL-6- or saline (*$p = 0.0405$) (Fig. 4F and Supplementary Fig. 10H–J). These observations indicate that social stress causes direct

passage of the pro-inflammatory cytokine IL-6, which then acts directly within the NAc to induce depression-like behaviors.

Discussion

Overall, our findings suggest that chronic social stress alters BBB integrity through downregulation of the tight junction protein cldn5 in the NAc which, combined with stress-induced recruitment of peripheral immune signals, results in increased BBB permeability and passage of blood circulating proteins such as IL-6 and the development of depression-like behaviors (Supplementary Fig. 11). Our findings complement decades of correlative clinical evidence suggesting that the immune system and elevations in circulating pro-inflammatory cytokines, particularly IL-6, are involved in the establishment of MDD[1, 7, 11, 38, 39]. We previously reported higher serum IL-6 in untreated patients with MDD and treatment-resistant MDD when compared to healthy controls[11]. Though a potential link between BBB leakiness and depression was first proposed over 50 years ago[40], the development of new tools, such as valid rodent models of depression and high resolution imaging, have made it feasible to address this important question. Our work highlights an important functional role for BBB-related tight junction protein cldn5 as a novel regulator of stress-induced depression-like behaviors. While size-selective loosening of the BBB to small molecules (< 800 Da) was previously described in cldn5-deficient mice[23], we show for the first time that chronic social stress can also loosen the BBB by downregulating cldn5, allowing for larger molecules to infiltrate the NAc parenchyma in SS mice.

Though we found increased passage of large proteins of up to ~69kD, we did not detect infiltration of peripheral ccr2+ monocytes as in previous reports[14]. This may be related to differences in social stress paradigms or to our use of a bitransgenic mouse model that allows for simultaneous tracking of monocytes and microglia without generating chimeric mice through bone marrow transplantation. We nevertheless confirm a recent report showing that monocytes are recruited to vessels and ventricular space within the brain[34]. From these vascular sites, monocytes can release pro-inflammatory cytokines, such as IL-6, that can then penetrate the brain parenchyma to act locally on neurons and glia. To our knowledge, this is the first study to provide direct evidence that chronic stress is sufficient to allow infiltration of circulating cytokines in the absence of local mechanical trauma or a brain tumor[41, 42]. Greater understanding of the mechanisms by which chronic stress activates the immune system and undermines BBB integrity may promote the design of more effective antidepressant strategies, either by augmenting current treatment protocols or by informing the discovery of new therapeutics that enhance neurovascular health within stress-related brain regions. A major impediment to this goal will be the development of novel therapeutic agents that can enhance Cldn5 expression in order to repair endothelial damage as, to date, no such compound exists.

Online Methods

Mice

Male C57BL/6J mice (~25 g) were purchased at 7 weeks of age from the Jackson Laboratory and allowed one week of acclimation to the Icahn School of Medicine at Mount

Sinai (ISMMS) housing facilities before the start of experiments. *ccr2*^{RFP}:: *cx3cr1*^{GFP} mice were bred at the ISMMS facilities and used at 8–10 weeks of age. Sexually experienced retired male CD-1 breeders (~40 g) of at least 4 months of age were purchased from Charles River Laboratories and used as aggressors (AGG). All mice were single housed following CSDS and maintained on a 12-h/12-h light/dark cycle throughout. Mice were provided with *ad libitum* access to water and food except during the novelty-suppressed feeding test. Behavioral assessments and tissue collection were performed into the dark phase. All mouse procedures were performed in accordance with the National Institutes of Health Guide for Care and Use of Laboratory Animals and the ISMMS Animal Care and Use Committee.

Chronic social defeat stress (CSDS)

CSDS was performed as previously described[11, 27, 32]. CD-1 mice were screened for aggressive behavior during inter-male social interactions for three consecutive days on the basis of previously described criteria[27, 43], and housed within the social defeat cage (26.7 cm width × 48.3 cm depth × 15.2 cm height, Allentown Inc) 24 h before the start of defeats (day 0) on one side of a clear perforated Plexiglas divider (0.6 cm × 45.7 cm × 15.2 cm, Nationwide Plastics). Experimental C57Bl/6J or *ccr2*^{RFP}:: *cx3cr1*^{GFP} mice were subjected to physical interactions with a novel CD-1 AGG for 10 min once per day over 10 consecutive days. After antagonistic interactions, experimental mice were removed and housed on the opposite side of the social defeat cage divider allowing sensory contact over the subsequent 24-h period. Unstressed control mice were housed two per cage in each side of a perforated divider and rotated daily in a similar manner without being exposed to the CD-1 AGG mice. Experimental mice were single housed after the last bout of physical interaction and social interaction (SI) test was conducted 24-h later.

Microdefeat stress

A subthreshold variation of the CSDS protocol was used to evaluate increased susceptibility to stress[11, 32]. Experimental C57Bl/6J mice were exposed to physical interactions with a new CD-1 AGG for three consecutive bouts of 5 min, with 15 min rest period between each bout. SI test was conducted 24 h later.

Social interaction/avoidance test

SI testing was performed as previously described under red-light conditions[11, 27, 32]. First, mice were placed in a Plexiglas open-field arena (42 cm × 42 cm × 42 cm, Nationwide Plastics) with a small wire animal cage placed at one end. Movements were monitored and recorded automatically for 2.5 min with a tracking system (Ethovision 11.0 Noldus Information Technology) to determine baseline exploratory behavior and locomotion in the absence of a social target (AGG). At the end of 2.5 min, the mouse was removed and the arena cleaned. Next, exploratory behavior in the presence of a novel social target inside the small wire animal cage was measured for 2.5 min and time spent in the interaction/corner zones and overall locomotion was compared. SI ratio was calculated by dividing the time spent in the interaction zone when the AGG was present divided by the time spent in the interaction zone when the AGG was absent. All mice with a SI ratio below 1.0 were classified as stress-susceptible (SS) and all mice with a SI ratio above 1.0 were classified as resilient (RES).

Splash test

The splash test was used to compare grooming behavior in stressed versus unstressed virus-injected mice under red-light conditions as described previously[31]. A 10% sucrose solution was sprayed on the lower back of the mice and time spent grooming was videotaped and then calculated with a stop watch.

Sucrose preference test

Anhedonic responses of stressed versus unstressed virus-injected mice was evaluated with a standard sucrose preference assay. Water bottles from home cages were removed and replaced with two 50-mL conical tubes with sipper tops filled with water for a 24-h habituation period. Next, water from one of the 50-mL conical tube was replaced with a 1% sucrose solution. All tubes were weighed and mice were allowed to drink *ad libitum* for a 24-h period. Tubes were then reweighed and switched for another 24-h period of *ad libitum* drinking to prevent place preference. At the end of the 48-h testing, sucrose preference was calculated by dividing the total amount of sucrose consumed by the total amount of fluid consumed over the two days of sucrose availability.

Forced swim test

Mice were placed into a 4-L glass beaker filled with 3 L of water at 25°C under bright light conditions and videotaped for 6 min. Time spent immobile was measured with a stop watch. Immobility was defined as no movement at all or only minor movements necessary to keep the nose above the water versus mobility, which was defined by swimming and struggling behaviors.

Novelty-suppressed feeding

This test assesses stress-induced anxiety by measuring aversion to feed in a novel environment despite food deprivation. Virus-injected stressed or unstressed mice were food-deprived overnight (with *ad libitum* access to water) and then placed in the corner of a novel white Plexiglas arena (42 cm × 42 cm × 42 cm, Nationwide Plastics) with the floor covered in corn cob bedding under red-light conditions. A food pellet was previously positioned in the middle of the arena. Latency to eat was measured with a stopwatch and defined by the first bite into the food pellet. Maximum time allowed was set at 10 min.

Elevated plus maze

Mice were placed in a black Plexiglas cross-shaped elevated plus maze (arms of 12 cm width × 50 cm length) under red-light conditions for 5 min. The maze consists of a center area, two opens arms with no wall and two closed arms with 40-cm high walls set on a pedestal 1 m above floor level. Locomotion was monitored and tracked using an automated system (Ethovision 11.0 Noldus Information Technology).

Open Field

Mice were placed in a white Plexiglas open-field arena (42 cm × 42 cm × 42 cm, Nationwide Plastics) and locomotion was monitored and tracked using an automated system (Ethovision 11.0 Noldus Information Technology) for 10 min. An area of 10 cm × 10 cm

was defined as the center and an adjacent 20 cm × 20 cm area was defined as the middle. The area along the walls was defined as the periphery.

Transcriptional profiling

Nucleus accumbens (NAc), hippocampus (HIPP) or prefrontal cortex (PFC) samples were collected and processed as described previously[32]. Bilateral 14-gauge punches were collected from 1-mm coronal slices on wet ice after rapid decapitation and immediately placed on dry ice and stored at −80°C until use. RNA was isolated using TRIzol (Invitrogen) homogenization and chloroform layer separation. The clear RNA layer was processed with RNAeasy MicroKit (Qiagen), analyzed with NanoDrop (Thermo Fisher Scientific) and 500 ng of RNA was reverse transcribed to cDNA with qScript (Quanta Biosciences). Resulting cDNA was then diluted to 500 µl and 3 µl was used for each quantitative PCR reaction with 5 µl of Perfecta SYBR Green (Quanta Biosciences), forward/reverse primers (0.5 µl each or 1 µl for PrimeTime® qPCR primers) and 1 µl of water. Samples were heated to 95°C for 2 min followed by 40 cycles of 95°C for 15 s, 60°C for 33 s ad 72°C for 33 s. Analysis was done using the ΔΔC(t) method and samples were normalized to *gapdh* (mouse) or *GAPDH* (human) housekeeping gene. Primer pairs are listed in Supplementary Information Table 1, 3 and 4 (Integrated DNA technologies).

Immunohistochemistry (IHC) and quantification of tight junction protein levels

Mice were anesthetized with a mixture of ketamine (100 mg/kg of body weight) and xylazine (10 mg/kg of body weight), perfused for 7 min with 0.1 M PBS and the brains quickly extracted and frozen in OCT Compound (Fisher Scientific) using isopentane on dry ice. Immunostaining was performed according to Mishra et al.,[44] with minor modifications. Briefly, blocks were stored at −20°C for 24 hours before slicing on a cryostat at 12-µm-thickness. Slices were post-fix for 10 min in ice cold methanol before a quick wash in 0.1 M PBS. Sections were then incubated for 2 hours in 5% normal donkey serum (NDS) in 0.1 M PBS before overnight incubation with primary antibodies[45–47] (rabbit anti-cldn5, 1:100, Life Technologies, #34–1600; rabbit anti-occludin, 1:250, Life Technologies, #40–4700; rabbit anti-ZO-1, 1:50; Life Technologies, #61–7300) in 1% NDS in 0.1 M PBS. Double immunostaining with CD31 (anti-rat-CD31, 1:150, BD Biosciences, #5550274) was performed to allow localization of blood vessels for quantification of tight junctions protein levels. After three washes in PBS for 10 min, sections were incubated with anti-rabbit-Cy2 and anti-rat-Cy5 secondary antibodies for 2 h (1:400, Jackson Immunoresearch), washed again three times with PBS and stained with 4,6-diamidino-2-phenylindole (DAPI) to visualize nuclei. Slices were mounted and cover slipped with ProLong Diamond Antifade Mountant (Invitrogen). One-µm-thick z-stack images of the NAc, HIPP or PFC were acquired on a LSM-780 confocal microscope (Carl Zeiss). Images were taken using a 40× lens with a resolution of 1056 × 288 and a zoom of 2.0. Pixel size was 0.1 µm in the x-y-z planes, pixel dwell time was 1.58 µs and the line average was set at 2. Flattened z-stack average intensity was compared using Image J (NIH) with the region or interested (ROI) defined using CD31 staining.

IHC for Evans Blue (EB)

Perivascular marker isolectin B4 (Ib4) and intravascular Evans blue (EB) staining were performed as previously described[48] followed by cldn5 indirect immunostaining[33]. Mice were anesthetized with a mixture of ketamine (100 mg/kg of body weight) and xylazine (10 mg/kg of body weight) and administered 6 μl/g of body weight 2% (wt/vol) EB (Sigma) dissolved in saline through retro-orbital injection. After 10 min, the mouse was decapitated and the brain was collected and fixed in 15-mL freshly prepared, cold 4% paraformaldehyde (PFA) + 0.05% glutaraldehyde. Brains were then cryoprotected in 30% sucrose, frozen and sliced on a cryostat at 40-μm-thickness. Slices were washed in 0.1 M phosphate buffered saline (PBS) and antigen retrieval was performed as described in[48] before incubation for 72 h at 4°C with biotinylated-Ib4 (1:50, Sigma) in $CaCl_2$-containing buffer and blocking solution (0.05% Triton X-100 and 2% NDS). After three washes in PBS for 10 min, sections were incubated with streptavidin-Cy3 (1:500, Sigma) secondary antibody in $CaCl_2$-containing buffer and blocking solution (0.05% Triton X-100 and 2% NDS) for 24 h. Sections were washed again three times with PBS and stained DAPI to visualize nuclei. Slices were mounted and cover slipped with ProLong Diamond Antifade Mountant (Invitrogen). Ten-μm-thick z-stack images of the NAc, HIPP or PFC were acquired on a LSM-780 confocal microscope (Carl Zeiss). Images were taken using a 40× lens with a resolution of 1056 × 288 and a zoom of 2.0. Pixel size was 0.1 μm in the x-y-z planes, pixel dwell time was 1.58 μs and the line average was set at 2.

Capillary extraction and Western Blot

For whole homogenate sample, a half brain of a naïve mouse was collected and homogenized in a RIPA lysis buffer (Sigma) containing phosphatase and protease inhibitor cocktails (Sigma). For capillary extraction, half brain of a naïve mouse was homogenized in 1 mL of cold DMEM using a Dounce homogenizer and then centrifuged at 4,000 g for 5 min at 4°C. The supernatant was removed and the pellet was resuspended in 18% dextran solution diluted in 0.1 M PBS as previously described[49]. After centrifugation (6,000 g for 10 min at 4°C), the supernatant and myelin debris floating at the surface were removed. The pellet was resuspended in DMEM supplemented with 1 mg/mL collagenase/dispase, 40 μg/mL DNase 1 and 0.147 μg/mL tosyllysine chloromethyl ketone (Sigma), and incubated at 37°C for 75 min with agitation to free endothelial cells from pericytes, perivascular macrophages and remains of the basement membrane. After centrifugation (4,000 g for 10 min at room temperature), the supernatant was discarded and the pellet was resuspended in RIPA lysis buffer. All samples were centrifuged at 14,000 rpm for 30 min at 4°C before protein quantification with Microplate BCA Protein Assay Kit (Bio-Rad Laboratories). Equal amounts of protein samples were separated by SDS-PAGE (Bio-Rad 4–20% polyacrylamide gels) and transferred to PVDF membranes (Bio-Rad). The membranes were blocked with 5% bovine serum albumin (BSA) in 0.1 M PBS and incubated overnight with primary antibodies against cldn5 (1:1,000, rabbit, Life Technologies, #34–1600), glial fibrillary acidic protein, gfap (1:1,000, guinea pig, Synaptic Systems, #173 004) or neun (1:1,000, mouse, Millipore, MAB377). After four 10-min washes with Tris Buffer Saline supplemented with Tween 20 (TBST), membranes were incubated for 2-h with secondary antibodies (1:5000, Vector Laboratories, goat anti-rabbit #PI-1000, Life Technologies, goat anti-mouse #G-21040, goat anti-guinea pig, #A18769). Membranes were washed four more

times with TBST and then antibody binding was detected using SuperSignal West Dura Supplementary Duration Substrate (Thermo Fisher Scientific) and a Bio-Rad Molecular Imager ChemiDoc™ XRS detection system with Image Lab software. Quantification was performed with Image J (NIH).

For virus validation, bilateral NAc punches were combined and homogenized in a RIPA lysis buffer (Sigma) containing phosphatase and protease inhibitor cocktails (Sigma). All samples were centrifuged at 14,000 rpm for 30 min at 4°C before protein quantification with DCA Protein Assay Kit (Bio-Rad Laboratories). Equal amounts of protein samples were separated by SDS-PAGE (Bio-Rad 4–20% polyacrylamide gels) and Western Blot for cldn5 and actin were performed as described above. Full-length Western Blots are available on Supplementary Fig. 2 and 12.

Imipramine treatment

Following SI test, unstressed CTRL and SS mice were randomly divided into either vehicle or imipramine treatment groups. Each mouse received daily i.p. injections of imipramine (20 mg/kg of body weight) or vehicle for 35 days[32]. All mice were screened again for social avoidance before tissue collection. Mice were then sacrificed 24-h after the last injection and bilateral 14-gauge NAc tissue punches were collected from 1-mm-thick coronal slices for quantitative PCR as described previously.

Transmission electron microscopy (TEM)

Mice were screened for behavioral phenotype with the SI test (CTRL, SS or RES) after 10-day CSDS and TEM was performed. Mice were administered horseradish peroxidase type II (HRP, Sigma, 100 mg/mL in PBS, 10 mg/20 g of body weight) through retro-orbital injection 24-h after SI test screening. HRP was allowed to circulate for 2 h and animals were overdosed using 100 mg/kg sodium pentobarbital, and transcardially perfused using ice cold 0.1 M PBS (pH 7.3) at a flow rate of 7.5 – 8 mls/min for 60 sec (until liver was completely cleared) followed with 2.5% glutaraldehyde in 0.1 M PBS (pH 7.3) for 12 min at a flow rate of 7.5 – 8 mls/min. Brains were removed, postfixed in same fixative above and stored at 4°C until ready for IHC. For morphology studies, samples were washed in 0.1M Sodium Cacodylate buffer, post-fixed in 1% Osmium Tetroxide/0.1M Cacodylate buffer, washed and dehydrated through a graduated Ethanol to Propylene Oxide series, and resin infiltrated with Epon (Electron Microscopy Sciences). Material was vacuum oven polymerized at 60°C for 48 hours. Semi-thick (1-μm) Toluidine Blue sections were used to identify the final ROI. Ultrathin sections (80 nm) were cut with a diamond knife (Diatome) with sections collected on 300 mesh copper grids (Electron Microscopy Sciences). Sections were counter-stained with uranyl acetate and lead citrate. For BBB permeability assessment, HRP-diaminobenzidine reaction (Vector Laboratories) was performed for 5 min on 200-μm coronal slices sectioned using a Vibratome (Leica, VT1000S). Reacted tissue was embedded as previously described[50]. Briefly, slices were cryoprotected via graded PB/glycerol (10, 20 and 30%) washes at 4°C, and manually microdissected to obtain blocks containing the ROI. Blocks were rapidly freeze-plunged into liquid propane cooled by liquid nitrogen (−90° C) in a Universal Cryofixation System KF80 (Reichert-Jung) and subsequently immersed in 1.5% uranyl acetate dissolved in anhydrous methanol at −90° C for 24 h in a

cryosubstitution unit (Leica). Block temperatures were raised from −90°C to −45°C in steps of 4°C/h, washed with anhydrous methanol, and infiltrated with Lowicryl resin (Electron Microscopy Sciences) at −45°C. The resin was polymerized by exposure to ultraviolet light (360 nm) for 48 h at −45°C followed by 24 h at 0°C. Using an EMUC7 ultramicrotome (Leica Microsystems Inc.), block faces were trimmed using a histo-knife (Diatome), and semi-thick (1-μm) Toluidine Blue sections were used to identify the final ROI. Ultrathin sections (90 nm) were cut with a diamond knife (Diatome) and sections collected on formvar/carbon coated nickel slot grids (Electron Microscopy Sciences). Images were taken using a Hitachi 7000 electron microscope (Hitachi High-Technologies Corporation America, Inc.) and imported to Photoshop for final brightness/contrast adjustment and sizing. Quantification was performed using Image J software (NIH). All blood vessels on the sample were imaged at a low and high magnification, with a total minimum of 100 images per animal (grid) sampled.

Human postmortem tissue collection

Whole-tissue NAc, HIPP or PFC (BA25) resections were collected and provided by the Quebec Suicide Brain Bank at the Douglas Hospital Research Center (McGill University) under approval of the institution Ethics Committee for the Montreal cohort[32]. For the Texas cohort, whole-tissue NAc resections were collected and provided by the Dallas Brain Collection (tissue was collected by the Dallas Medical Examiner's Office and the University of Texas Southwestern's Tissue Transplant Program) under approval of the University of Texas Southwestern Institutional Review Board[32]. Brain tissue was collected at local medical examiners offices after obtaining permissions. Blood toxicology was performed to exclude subjects using illicit drugs or psychotropic medications. Subjects with knock history of neurological disorders or head injury were also excluded. Demographic characteristics associated with each sample are listed in Supplementary Information Table 2. Clinical records and interviews were obtained for each case and reviewed by three to four mental health professionals to establish independent diagnoses followed by a consensus diagnosis in line with the Diagnostic and Statistical Manual of Mental Disorders (DSM) IV criteria. Cohorts were matched as closely as possible for gender, age, race, pH, postmortem interval and RNA integrity number[32].

Stereotaxic surgery and viral gene transfer

All surgeries were performed under aseptic conditions using anesthetic as described previously[32]. Mice were anesthetized with a mixture of ketamine/xylazine, as mentioned in the IHC section, and positioned in a small animal stereotaxic instrument (David Kopf Instruments). The skull surface was exposed and 30-gauge syringe needles (Hamilton Co.) were used to bilaterally infused 0.5 μl of virus (1.0×10^{11} infectious unit/mL) expressing either AAV2/9-shRNA or AAV2/9-shRNA-*cldn5*[33] into the NAc (bregma coordinates: anteroposterior +1.6 mm, mediolateral +1.5 mm, dorsoventral −4.4 mm) or HIPP (bregma coordinates: anteroposterior −2.0 mm, mediolateral +1.0 mm, dorsoventral −2.2 mm) at a rate of 0.1 μl/min. All mice were allowed to recover for 2 weeks before activation of the viruses with doxycycline treatment (2 mg/mL in drinking water). Placement was validated with visualization of blood vessels with EB, green fluorescent protein (gfp) and cldn5 IHC. Briefly, virus-injected mice were anesthetized and retro-orbital injection of EB was

performed as described in the IHC section. Brains were collected after 10-min, fixed overnight, cryoprotected with 30% sucrose, frozen and 50-μm-thickness slices produced on a brain vibratome. After a quick wash in 0.1 M PBS, slices were transferred to blocking solution (2% NDS and 0.05% Triton X-100 in 0.1 M PBS) for 2 h before overnight incubation in primary antibody solution (anti-rabbit cldn5, 1:250; anti-chicken gfp, 1: 1,000, Aves in 2% NDS and 0.05% Triton X-100 in 0.1 M PBS). After three washes in 0.1 M PBS for 10 min, sections were incubated with anti-rabbit-Cy3 and anti-chicken-Cy2 secondary antibodies in 0.1 M PBS for 2 h (1:400, Jackson Immunoresearch), washed again three times with PBS and stained with DAPI. Slices were mounted and cover slipped with ProLong Diamond Antifade Mountant (Invitrogen).

Magnetic resonance imaging (MRI) scans

Following 10-day CSDS and SI behavioral screening, blood-brain barrier (BBB) permeability was analyzed using a small rodent Bruker Biospec 7T/30 scanner system located at the Translational and Molecular Imaging Institute (TMII) at Mount Sinai Hospital (Details are included in the MRI Studies Reporting Summary). Mice were imaged under isoflurane anesthesia (5% in air for induction and 1.5% maintenance with 2 l/min flowrate). Baseline T1-weighed images were acquired using a FLASH sequence (32 slices, thickness 0.5mm, in-plane resolution (78mmx78mm). Gadolinium contrasting-agent Gd-DTPA was then administered through retro-orbital injection. The concentration was 0.3mmol/kg and a bolus of 0.1ml was injected. The animals were then rescanned using the same T1 protocol 25 minutes after injection. Images were analyzed using in-house software developed under Matlab V2015b (Mathworks Inc., Natick, MA). Regions of interest (ROIs) were manually defined on the images and mean image intensities were extracted. Signal enhancement was defined as (Post-Pre)/Post. Paired t-tests were performed for the different ROIs.

Detection of injected tracers

Tracers were administered through retro-orbital injection in anesthetized animals (mixture of ketamine/xylazine) following 10-day CSDS and SI test screening. Quantification of BBB-related dyes was performed using unbiased extraction assays as described previously[51] with slight modifications to apply the protocol to specific brain regions instead of the entire brain. Briefly, EB (Sigma, 2% wt/vol, 6 μl/g of body weight) was allowed to circulate for 10 min in non-perfused animals used for IHC or 16 hours followed by 5-min intra-cardiac perfusion with 0.1 M PBS in mice used for comparative EB infiltration (IHC) and quantification. After perfusion the brain was removed and bilateral NAc, hippocampus and PFC punches were collected from 1-mm-thick coronal slices in 1.5 mL Eppendorf tubes previously weighed. Eppendorf tubes containing samples were weighed again before adding 100 μl pure dimethylformamide to each tube. Extraction was performed at 55°C for 72 hours. The samples were centrifuged at 21,000 g for 30 min and the supernatant collected. EB fluorescence of each sample was obtained on a SpectraMax 340PC384 microplate reader (Molecular Devices) and calculated from a serial dilution fluorescence curve using SoftMax Pro 5.2 software. A kidney lysate was used as a positive control.

Similarly, cadaverine conjugated to Alexa Fluor-555 (Life Technologies) was administered through retro-orbital injection and allowed to circulate for 2 hours in unstressed control and

defeated mice. For quantification, anesthetized animals were perfused for 5 min with 0.1 M PBS then bilateral NAc, hippocampus and PFC punches were collected in previously weighed Eppendorf tubes for tracer extraction. Samples were weighed, homogenized in 1% Triton X-100 in 0.1 M PBS and centrifuged at 16,000 rpm for 20 min. Relative fluorescence of the supernatant was measured on a SpectraMax 340PC384 microplate reader (Molecular Devices) and calculated from a serial dilution fluorescence curve using SoftMax Pro 5.2 software.

Isolation of brain leukocytes and flow cytometry

Mice were deeply anesthetized with a lethal dose of choral hydrate and transcardially perfused with 0.1 M PBS. Brain was removed and one forebrain hemisphere (without olfactory bulb) was minced, incubated in phenol-red free DMEM supplemented with 2% heat inactivated FBS, 10mM HEPES and Collagenase type IV (0.4 mg/mL) for 15 min and then passed through a 19G blunt syringe to obtain a homogeneous cell suspension. Mononuclear cells were separated with a 40% Percoll gradient. Isolated cells were surface stained in FACS buffer for 20–30 min on ice with the following antibodies: CD11b (clone M1/70, eBioscience), F4/80 (clone CI: A3-1, BioRad), CD45 (clone 30F11, eBioscience), MHC II (clone M5/114.15.2, eBioscience), CD3e (clone 145-2C11, Biolegend), Gr-1 (clone RB6–8C5, Biolegend), CD115 (clone AFS98, eBioscience). Multiparameter analysis was performed on a LSR II Fortessa (BD) and analyzed with FlowJo software (Tree Star) (Details are included in the Flow Cytometry Reporting Summary). Dead cells and doublets were excluded from all analysis.

IL-6 biotinylation

Recombinant Mouse IL-6 (RMIL6I, Thermo Fisher Scientific) was dissolved in 0.1 M sodium bicarbonate buffer, pH 7.5 and biotin-X SE (6-((Biotinoyl)Amino)Hexanoic Acid, Succinimidyl Ester (Biotinamidocaproate, *N*-Hydroxysuccinimidyl Ester)) in dimethylsulfoxide. Conjugation of biotin with IL-6 was performed at pH 7.5 with a 2:1 molar ratio, respectctively, by slowly adding biotin to the vortexing protein solution followed by incubation for 60 min at room temperature with continuous agitation. Conjugated IL-6-biotin (~21.45 kDa) was separated from unbound biotin (~0.45 kDa) using high-performance size-exclusion chromatography resin Zeba™ Spin Desalting Columns, 7K MWCO, 0.5 mL (Thermo Fisher Scientific), which is characterized by 95% retention/removal of salts and other small molecules (<1 kDa) and recovery of proteins and other macromolecules (>7 kDa). The conjugate was diluted in saline solution to a final concentration of 20 μg/ml. Biotinylated IL-6 (20 ng diluted in saline solution) was administered through retro-orbital injection in CTRL, SS or RES mice 24h after SI test screening and allowed to circulate for 2 h. The mice were then anesthetized with a mixture of ketamine/xylazine, perfused with 0.1 M PBS for 5 min and the brain was collected and fixed overnight in 4% PFA. Brains were cryoprotected with 30% sucrose, frozen and then sliced on the cryostat at a thickness of 40-μm. IL-6-biotin conjugate was detected with Oregon Green® 488 conjugate of NeurAvidin® biotin-binding protein (Thermo Fisher Scientific), a form of avidin that has been processed to remove carbohydrate and lower its isoelectric point substantially decreasing background due to nonspecific binding. Double labeling with perivascular marker CD31 (rat anti-CD31, 1:150, BD Biosciences, anti-rat-

Cy5, 1:400, Jackson Immunoresearch) was performed as described in the IHC section. After three washes with 0.1 M PBS, slices were stained with DAPI, mounted and cover slipped with ProLong Diamond Antifade Mountant (Invitrogen).

IL-6 i.p. injection and ELISA

Stress-naïve mice were administered saline solution, 5 or 15 ng/mL mouse recombinant IL-6 diluted in saline solution through i.p. injection 20 min before tissue collection. Blood serum and bilateral NAc punches were collected in 1-mm-thick coronal sections on wet ice and IL-6 levels were detected with a solid phase sandwich IL-6 ELISA (BD Biosciences). IL-6 levels were measured on a SpectraMax 340PC384 microplate reader (Molecular Devices) and calculated from a serial dilution curve using SoftMax Pro 5.2 software. Another cohort of mice went through 10-day CSDS and SI behavioral screening before blood serum, NAc, HIPP and PFC tissue collection and assessment of IL-6 levels by ELISA (R&D Systems).

Osmotic minipump surgery and IL-6 infusion

Mice were anesthetized with a mixture of ketamine/xylazine as described in the previous sections and surgically implanted with bilateral NAc guide cannulae (Plastic One). Cannulae (Plastics One) were delivered into the NAc according to bregma coordinates (anteroposterior +1.6 mm, mediolateral +1.5 mm, dorsoventral −4.4 mm) and fixed to the skull with Loctite skull adhesive (Henkel). Saline or a total of 5 ng of IL-6 (diluted at 10 ng/mL in saline solution) was administered over 5 min (0.1 mL /min) using a mini-pump (Harvard Apparatus), followed by a 20-min rest, before subthreshold micro-defeat stress. SI test was conducted 24h later. Mice were then sacrificed and perfused as described above in the IHC section to confirm placement of cannula in the NAc.

Statistical analysis

Sample size for CSDS mouse cohorts was calculated based on previous studies of CSDS and depression-like behaviors[11, 32] (Details are included in the Life Sciences Reporting Summary). Outliers for social interaction (SI) test screening were identified as being greater than two standard deviations from the mean and excluded. All mice were assigned to stress-susceptible (SS) or resilient (RES) groups based on their behavioral profile when compared to unstressed controls (CTRL). CTRL and SS mice were randomly assigned to vehicle or imipramine treatment groups using Excel spreadsheet random function. SI screening and behavioral tests were performed with automated tracking systems when possible. If not, scoring was done by experimenters blinded to experimental conditions (for splash test, sucrose preference test and forced swim test). Outliers for behavioral testing, for example characterized by impaired locomotion, were identified as being greater than two standard deviations from the mean and excluded from statistical analysis. One unstressed AAV-shRNA-*cldn5* mouse was excluded after verification of virus injection placement. All t-tests, one-way ANOVAs, two-way ANOVAs and Pearson's correlations were performed using GraphPad Prism software (GraphPad Software Inc.). Statistical significance was set at $*p < 0.05$. Bonferroni was used as a post-hoc test when appropriate for one-way and two-way ANOVAs and statistical significance was set at $*p < 0.05$. Visual representation of average and SEM with heat maps was done using Matlab-based software. Individual values were used to compute correlation matrices and p values were determined by Matlab-based

software. Normality was determined by Kolmogorov-Smirnov, D'Agostino-Pearson and Shapiro-Wilk normality tests using GraphPad Prism software. All quantitative PCR, immunohistochemistry and BBB-related tracer quantification were performed in duplicate in two different cohorts of mice.

Data Availability

The authors declare that all data supporting the findings of this study are available within the paper and supplementary information files.

Supplementary Material

Refer to Web version on PubMed Central for supplementary material.

Acknowledgments

This research was supported by Mental Health grants RO1 MH090264 (S.J.R.), P50 MH096890 (S.J.R.), P50 AT008661-01 (S.J.R.), RO1 MH114882 (S.J.R.), RO1 MH104559 (S.J.R. and M.M.), T32 MH087004 (M.L.P., M.H. and M.F.), T32 MH096678 (M.L.P.), F30 MH100835 (M.H.), F31 MH105217 (M.L.P.), a Janssen/IMHRO Rising Star Translational Research Award (S.J.R.), a Swiss National Science Foundation Advanced Postdoc Mobility fellowship (V.K.) and Brain and Behavior Research Foundation NARSAD young investigator award (G.E.H.). C.M. is supported by a Brain and Behavior Research Foundation NARSAD Young Investigator Grant sponsored by the P&S Fund. The authors would like to thank Dr. Annika Keller for her advice on BBB-related studies and the Center for Comparative Medicine and Surgery housing facilities staff for their work and support.

References

1. Menard C, Pfau ML, Hodes GE, Russo SJ. Immune and Neuroendocrine Mechanisms of Stress Vulnerability and Resilience. Neuropsychopharmacology. 2016; 42:62–80. [PubMed: 27291462]
2. Kessler RC, Chiu WT, Demler O, Merikangas KR, Walters EE. Prevalence, severity, and comorbidity of 12-month DSM-IV disorders in the National Comorbidity Survey Replication. Arch Gen Psychiatry. 2005; 62:617–627. [PubMed: 15939839]
3. Seligman F, Nemeroff CB. The interface of depression and cardiovascular disease: therapeutic implications. Ann N Y Acad Sci. 2015; 1345:25–35. [PubMed: 25809518]
4. Carney RM, Freedland KE. Depression and coronary heart disease. Nat Rev Cardiol. 2016; 14:145–155. [PubMed: 27853162]
5. Wood SK. Individual differences in the neurobiology of social stress: implications for depression-cardiovascular disease comorbidity. Curr Neuropharmacol. 2014; 12:205–211. [PubMed: 24669213]
6. Huffman JC, Celano CM, Beach SR, Motiwala SR, Januzzi JL. Depression and cardiac disease: epidemiology, mechanisms, and diagnosis. Cardiovasc Psychiatry Neurol. 2013; 2013:695925. [PubMed: 23653854]
7. Hodes GE, Kana V, Menard C, Merad M, Russo SJ. Neuroimmune mechanisms of depression. Nat Neurosci. 2015; 18:1386–1393. [PubMed: 26404713]
8. Barnes J, Mondelli V, Pariante CM. Genetic Contributions of Inflammation to Depression. Neuropsychopharmacology. 2016; 42:81–98. [PubMed: 27555379]
9. Dantzer R. Cytokine, sickness behavior, and depression. Immunol Allergy Clin North Am. 2009; 29:247–264. [PubMed: 19389580]
10. Miller AH, Raison CL. The role of inflammation in depression: from evolutionary imperative to modern treatment target. Nat Rev Immunol. 2016; 16:22–34. [PubMed: 26711676]
11. Hodes GE, et al. Individual differences in the peripheral immune system promote resilience versus susceptibility to social stress. Proc Natl Acad Sci U S A. 2014; 111:16136–16141. [PubMed: 25331895]

12. Powell ND, et al. Social stress up-regulates inflammatory gene expression in the leukocyte transcriptome via beta-adrenergic induction of myelopoiesis. Proc Natl Acad Sci U S A. 2013; 110:16574–16579. [PubMed: 24062448]
13. Heidt T, et al. Chronic variable stress activates hematopoietic stem cells. Nat Med. 2014; 20:754–758. [PubMed: 24952646]
14. Wohleb ES, Powell ND, Godbout JP, Sheridan JF. Stress-induced recruitment of bone marrow-derived monocytes to the brain promotes anxiety-like behavior. J Neurosci. 2013; 33:13820–13833. [PubMed: 23966702]
15. Weber MD, Godbout JP, Sheridan JF. Repeated Social Defeat, Neuroinflammation, and Behavior: Monocytes Carry the Signal. Neuropsychopharmacology. 2016; 42:46–61. [PubMed: 27319971]
16. Esposito P, et al. Acute stress increases permeability of the blood-brain-barrier through activation of brain mast cells. Brain Res. 2001; 888:117–127. [PubMed: 11146058]
17. Santha P, et al. Restraint Stress-Induced Morphological Changes at the Blood-Brain Barrier in Adult Rats. Front Mol Neurosci. 2015; 8:88. [PubMed: 26834555]
18. Friedman A, et al. Pyridostigmine brain penetration under stress enhances neuronal excitability and induces early immediate transcriptional response. Nat Med. 1996; 2:1382–1385. [PubMed: 8946841]
19. Sharma HS, Dey PK. Impairment of blood-brain barrier (BBB) in rat by immobilization stress: role of serotonin (5-HT). Indian J Physiol Pharmacol. 1981; 25:111–122. [PubMed: 7287133]
20. Niklasson F, Agren H. Brain energy metabolism and blood-brain barrier permeability in depressive patients: analyses of creatine, creatinine, urate, and albumin in CSF and blood. Biol Psychiatry. 1984; 19:1183–1206. [PubMed: 6498242]
21. Roszkowski M, Bohacek J. Stress does not increase blood-brain barrier permeability in mice. J Cereb Blood Flow Metab. 2016; 36:1304–1315. [PubMed: 27146513]
22. Gunzel D, Yu AS. Claudins and the modulation of tight junction permeability. Physiol Rev. 2013; 93:525–569. [PubMed: 23589827]
23. Nitta T, et al. Size-selective loosening of the blood-brain barrier in claudin-5-deficient mice. J Cell Biol. 2003; 161:653–660. [PubMed: 12743111]
24. Meltzer H, Vostanis P, Ford T, Bebbington P, Dennis MS. Victims of bullying in childhood and suicide attempts in adulthood. Eur Psychiatry. 2011; 26:498–503. [PubMed: 21310592]
25. Berton O, Nestler EJ. New approaches to antidepressant drug discovery: beyond monoamines. Nat Rev Neurosci. 2006; 7:137–151. [PubMed: 16429123]
26. Menard C, Hodes GE, Russo SJ. Pathogenesis of depression: Insights from human and rodent studies. Neuroscience. 2016; 321:138–162. [PubMed: 26037806]
27. Golden SA, Covington HE 3rd, Berton O, Russo SJ. A standardized protocol for repeated social defeat stress in mice. Nat Protoc. 2011; 6:1183–1191. [PubMed: 21799487]
28. Russo SJ, Nestler EJ. The brain reward circuitry in mood disorders. Nat Rev Neurosci. 2013; 14:609–625. [PubMed: 23942470]
29. Zhang Y, et al. An RNA-sequencing transcriptome and splicing database of glia, neurons, and vascular cells of the cerebral cortex. J Neurosci. 2014; 34:11929–11947. [PubMed: 25186741]
30. Zhang Y, et al. Purification and Characterization of Progenitor and Mature Human Astrocytes Reveals Transcriptional and Functional Differences with Mouse. Neuron. 2016; 89:37–53. [PubMed: 26687838]
31. Hodes GE, et al. Sex Differences in Nucleus Accumbens Transcriptome Profiles Associated with Susceptibility versus Resilience to Subchronic Variable Stress. J Neurosci. 2015; 35:16362–16376. [PubMed: 26674863]
32. Golden SA, et al. Epigenetic regulation of RAC1 induces synaptic remodeling in stress disorders and depression. Nat Med. 2013; 19:337–344. [PubMed: 23416703]
33. Campbell M, et al. Systemic low-molecular weight drug delivery to pre-selected neuronal regions. EMBO Mol Med. 2011; 3:235–245. [PubMed: 21374818]
34. McKim DB, et al. Microglial recruitment of IL-1beta-producing monocytes to brain endothelium causes stress-induced anxiety. Mol Psychiatry, in press. 2017

35. Saederup N, et al. Selective chemokine receptor usage by central nervous system myeloid cells in CCR2-red fluorescent protein knock-in mice. PLoS One. 2010; 5:e13693. [PubMed: 21060874]
36. Mizutani M, et al. The fractalkine receptor but not CCR2 is present on microglia from embryonic development throughout adulthood. J Immunol. 2012; 188:29–36. [PubMed: 22079990]
37. Ginhoux F, Jung S. Monocytes and macrophages: developmental pathways and tissue homeostasis. Nat Rev Immunol. 2014; 14:392–404. [PubMed: 24854589]
38. Maes M, et al. Increased serum IL-6 and IL-1 receptor antagonist concentrations in major depression and treatment resistant depression. Cytokine. 1997; 9:853–858. [PubMed: 9367546]
39. Dowlati Y, et al. A meta-analysis of cytokines in major depression. Biol Psychiatry. 2010; 67:446–457. [PubMed: 20015486]
40. Coppen AJ. Abnormality of the blood-cerebrospinal fluid barrier of patients suffering from a depressive illness. J Neurol Neurosurg Psychiatry. 1960; 23:156–161. [PubMed: 13811865]
41. Hambardzumyan D, Gutmann DH, Kettenmann H. The role of microglia and macrophages in glioma maintenance and progression. Nat Neurosci. 2016; 19:20–27. [PubMed: 26713745]
42. Shichita T, et al. Pivotal role of cerebral interleukin-17-producing gammadeltaT cells in the delayed phase of ischemic brain injury. Nat Med. 2009; 15:946–950. [PubMed: 19648929]
43. Golden SA, et al. Basal forebrain projections to the lateral habenula modulate aggression reward. Nature. 2016; 534:688–692. [PubMed: 27357796]
44. Mishra V, et al. Primary blast causes mild, moderate, severe and lethal TBI with increasing blast overpressures: Experimental rat injury model. Sci Rep. 2016; 6:26992. [PubMed: 27270403]
45. Keaney J, et al. Autoregulated paracellular clearance of amyloid-beta across the blood-brain barrier. Sci Adv. 2015; 1:e1500472. [PubMed: 26491725]
46. Campbell M, et al. RNAi-mediated reversible opening of the blood-brain barrier. J Gene Med. 2008; 10:930–947. [PubMed: 18509865]
47. Doyle SL, et al. IL-18 attenuates experimental choroidal neovascularization as a potential therapy for wet age-related macular degeneration. Sci Transl Med. 2014; 6:230ra244.
48. Walchli T, et al. Quantitative assessment of angiogenesis, perfused blood vessels and endothelial tip cells in the postnatal mouse brain. Nat Protoc. 2015; 10:53–74. [PubMed: 25502884]
49. Blank T, et al. Brain Endothelial- and Epithelial-Specific Interferon Receptor Chain 1 Drives Virus-Induced Sickness Behavior and Cognitive Impairment. Immunity. 2016; 44:901–912. [PubMed: 27096319]
50. Janssen WG, et al. Cellular and synaptic distribution of NR2A and NR2B in macaque monkey and rat hippocampus as visualized with subunit-specific monoclonal antibodies. Exp Neurol. 2005; 191(Suppl 1):S28–44. [PubMed: 15629759]
51. Armulik A, et al. Pericytes regulate the blood-brain barrier. Nature. 2010; 468:557–561. [PubMed: 20944627]

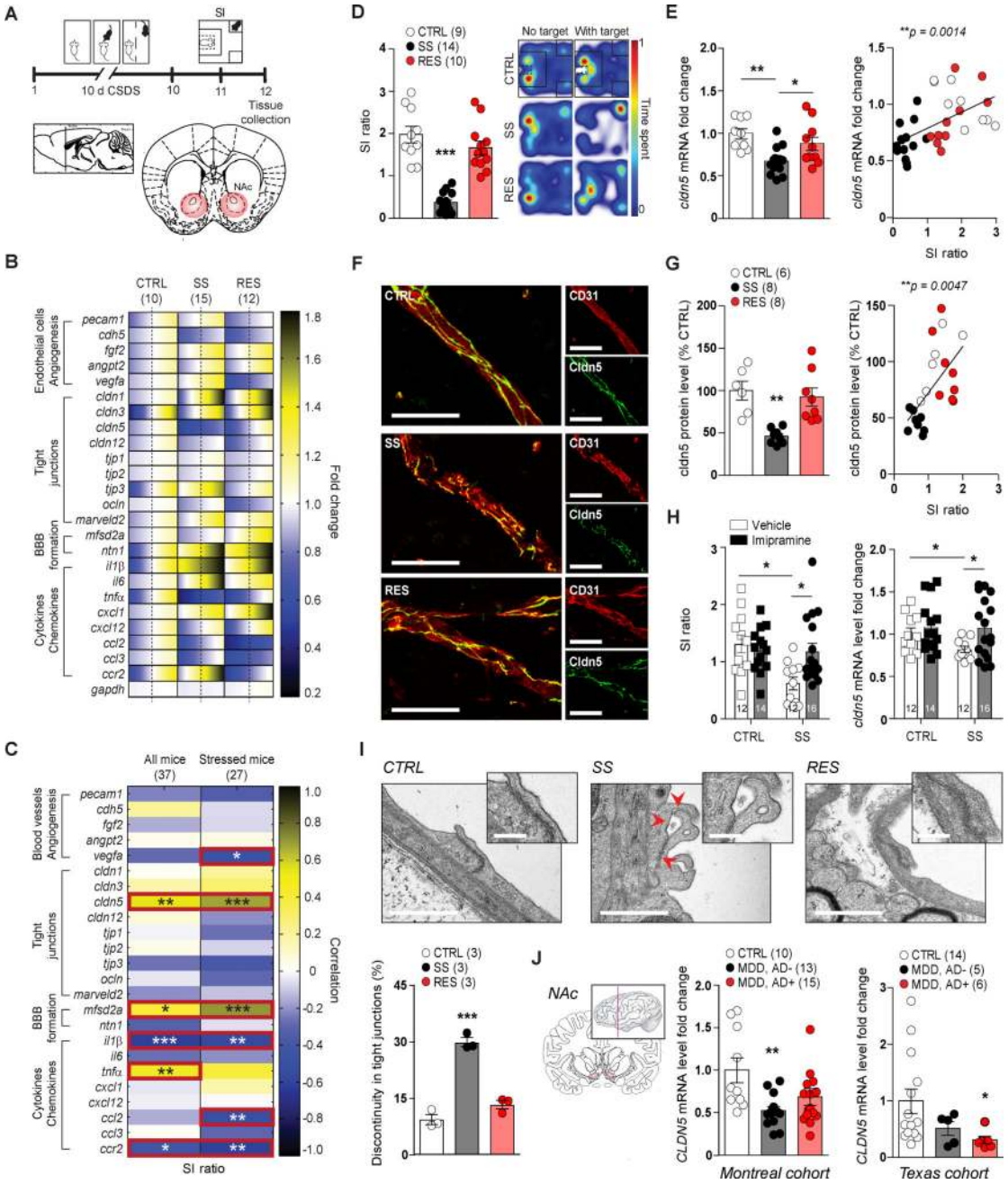

Figure 1. Social stress vulnerability and MDD is associated with reduced *cldn5* expression

A) Experimental timeline of 10-day social defeat stress (CSDS), social interaction (SI) behavioral screening and tissue collection of nucleus accumbens (NAc). **B)** Quantitative PCR revealed significant changes in the NAc of stress-susceptible (SS) and resilient (RES) mice when compared to unstressed controls (CTRL) for gene expression related to endothelial cell biology, angiogenesis, tight junctions, blood-brain barrier (BBB) formation and cytokines/chemokines. The range of color indicates individual differences within a group – standard error of the mean (SEM) from the average represented by the dashed line. **C)** Several patterns of gene expression correlated with SI ratio **(D)**. Representative heat

maps of SI test are shown on the right. Cldn5 mRNA **(E)** and protein **(F, G)** levels were lower in the NAc of SS mice and correlated with social avoidance. Scale bar is set at 20 μm. **H)** Chronic treatment with imipramine reversed social avoidance and rescued *cldn5* loss in SS mice. **I)** Transmission electron microscopy revealed discontinuity in tight junctions of SS (red arrows), but not resilient, mice. Scale bar is set at 500 nm (250 nm for insets), 52–66 tight junctions/mouse and three mice/group. **J)** *CLDN5* mRNA level was significantly lower in the NAc of MDD patients from two different cohorts. Data represent mean ± SEM, number of animals or patients (*n*) is indicated on graphs. Two-way ANOVA followed by Bonferroni's multiple comparison test for antidepressant treatment, correlations were evaluated with Pearson's correlation coefficient, and one-way ANOVA followed by Bonferroni's multiple comparison test for other graphs, $*p < 0.05$; $**p < 0.01$; $***p < 0.001$.

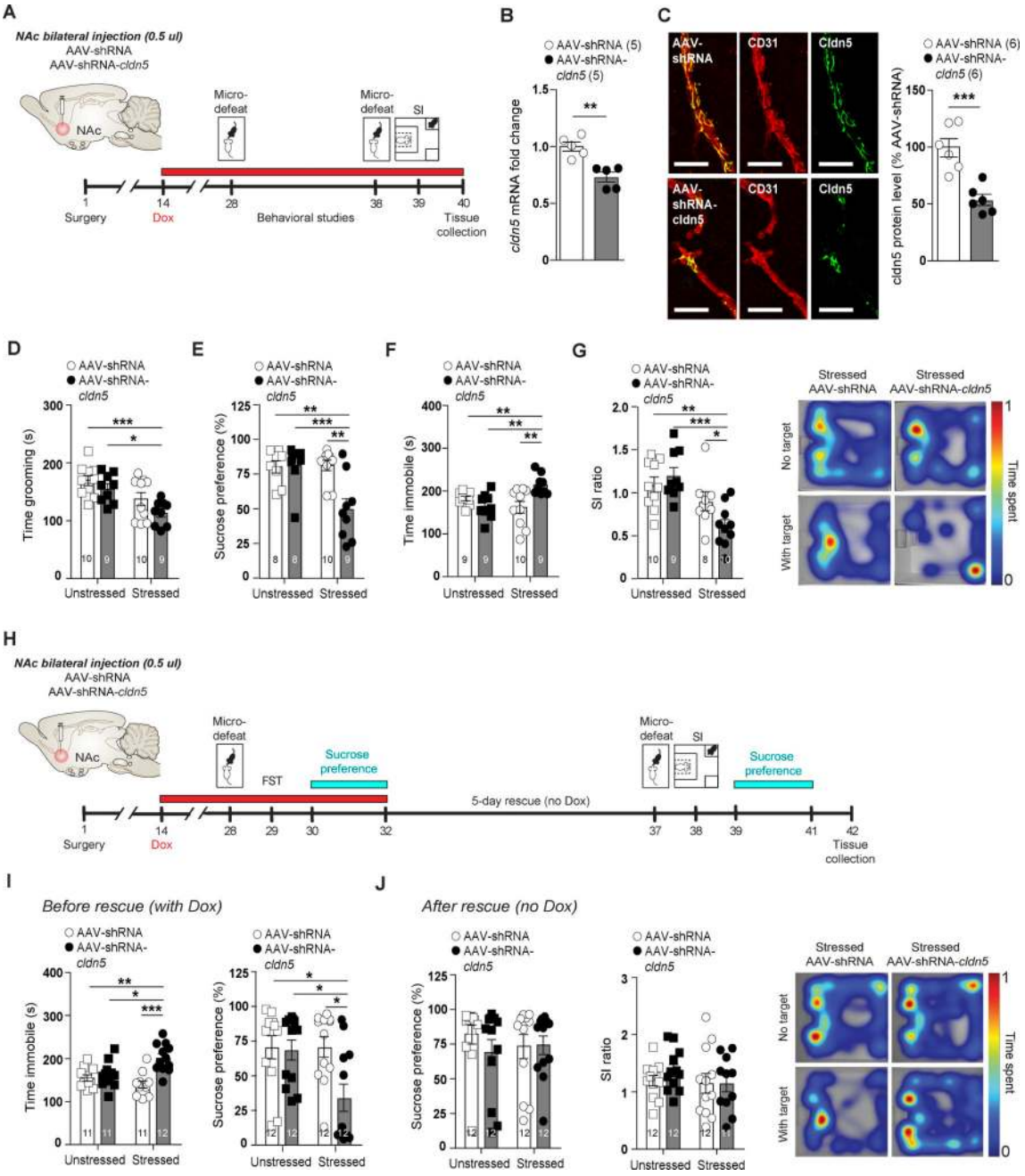

Figure 2. Conditional knockdown of cldn5 expression in the NAc is sufficient to induce depression-like behaviors

A) Experimental timeline of NAc bilateral injection of AAV-shRNA or AAV-shRNA-*cldn5* viruses and behavioral studies. Cldn5 mRNA **(B)** and protein **(C)** levels are reduced following AAV-shRNA-*cldn5* injection in the NAc of stress-naïve mice when compared to AAV-shRNA-injected animals. Co-staining with CD31 confirmed lower cldn5 protein level in blood vessels following AAV-shRNA-*cldn5* virus injection and doxycycline (Dox) treatment **(C)**. Scale bar is set at 2 μm. Downregulation of cldn5 expression prior to subthreshold micro-defeat (stressed) induced depression-like behaviors as assessed by splash

(D), sucrose preference **(E)**, forced swim **(F)** and social interaction **(G)** tests. The effect was significant when compared to unstressed mice and stressed AAV-shRNA. **H)** Experimental timeline of *cldn5* rescue experiment. **I)** Stressed AAV-shRNA-*cldn5* mice displayed depression-like behaviors when subjected to doxycycline treatment as assessed with forced swim test and sucrose preference. **J)** No difference was observed between groups for sucrose preference and social interaction when doxycycline was removed from the water, allowing normal cldn5 expression. Data represent mean ± SEM, number of animals (*n*) is indicated on graphs. Unpaired t-test for virus validation or two-way ANOVA followed by Bonferroni's multiple comparison test for behaviors, $*p < 0.05$; $**p < 0.01$; $***p < 0.001$.

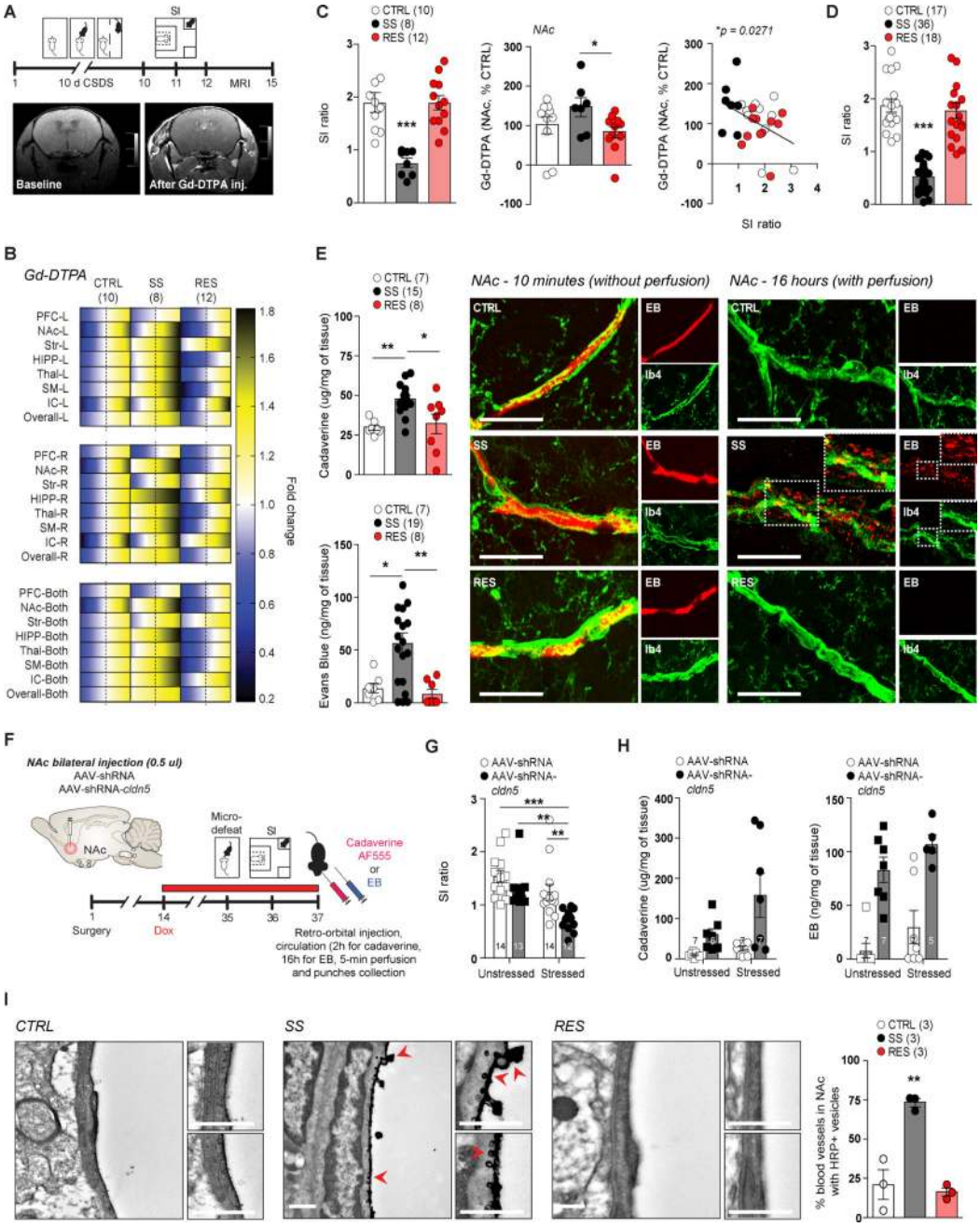

Figure 3. Social stress vulnerability is associated with increased blood-brain barrier (BBB) permeability

A) Experimental timeline of 10-day CSDS, SI screening, and magnetic resonance imaging (MRI) scans. Pictures display baseline MRI scan compared to 25 minutes after injection of the gadolinium-contrasting agent (Gd-DTPA). **B)** Higher Gd-DTPA signal was detected in different brain regions, including the NAc in SS mice and negatively correlated with SI ratio **(C)**. The range of color indicates individual differences within a group - SEM from the average represented by the dashed line. Assessment of BBB permeability with cadaverine Alexa Fluor-555 and Evans blue (EB) dyes revealed significant BBB leakiness in the NAc of

SS mice **(D, E)**. EB dye is present in all vessels within 10 min of injection and prior to perfusion **(E, left)** but can only be detected in the perivascular space of NAc blood vessels in SS mice after circulating 16 hours followed by 5-min perfusion **(E, right)**. Scale bar is set at 20 μm. **F, G)** Downregulation of cldn5 expression increased BBB permeability to cadaverine Alexa Fluor-555 and EB dyes **(H)** in AAV-shRNA-*cldn5* mice. **I)** Transmission electron microscopy, conducted 2 hours after injection of horseradish peroxidase (HRP) followed by 20-min perfusion, confirmed increased BBB permeability in the NAc of SS mice with HRP detected within the endothelial cell lining (red arrows). Quantification was performed on 34–61 blood vessels/mouse in three mice/group. Scale bar is set at 500 nm. Data represent mean ± SEM, number of animals (*n*) is indicated on graphs. Correlations were evaluated with Pearson's correlation coefficient, two-way ANOVA followed by Bonferroni's multiple comparison test for BBB permeability in virus-injected mice, one-way ANOVA followed by Bonferroni's multiple comparison test for other graphs, $*p < 0.05$; $**p < 0.01$; $***p < 0.001$.

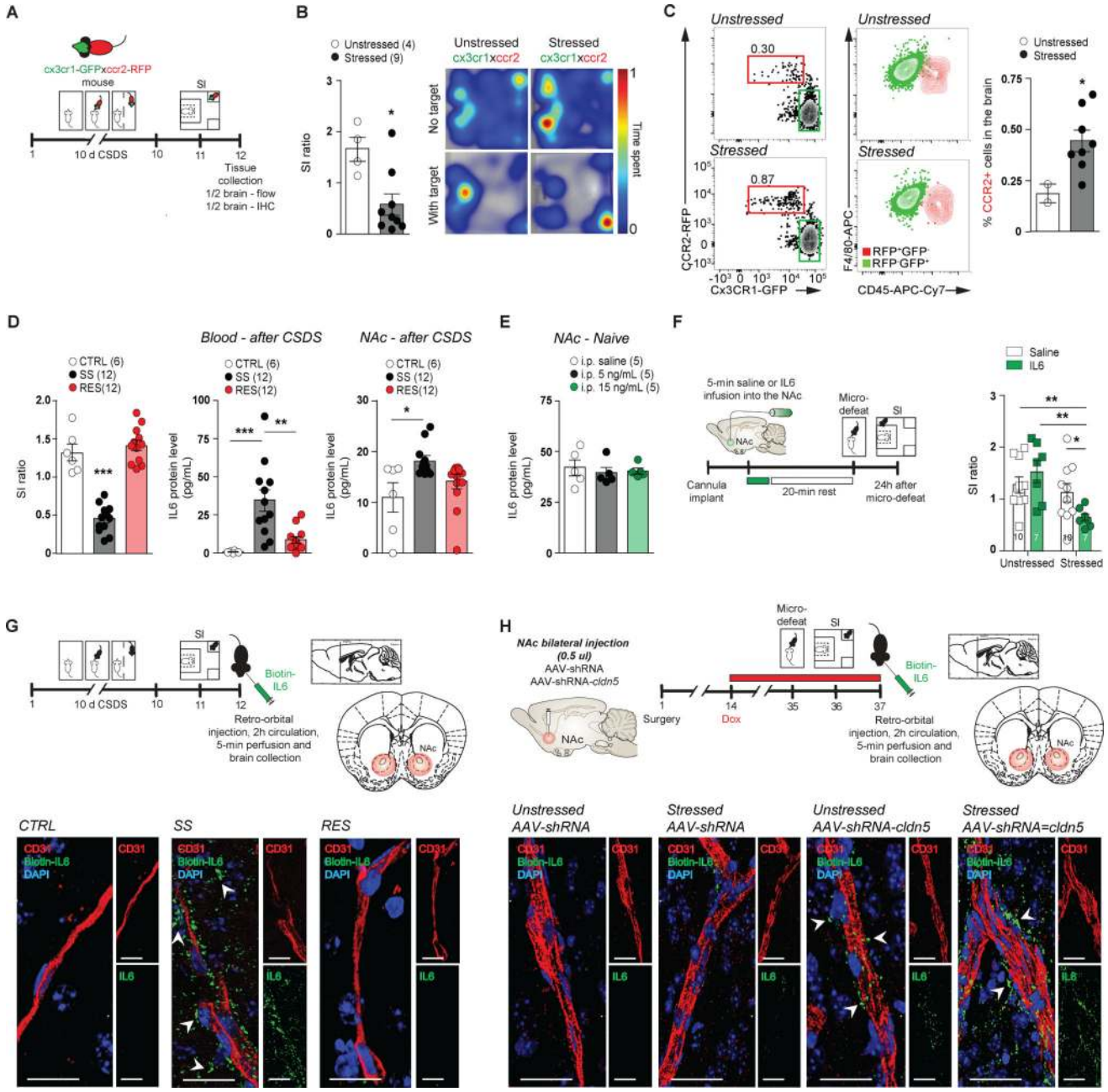

Figure 4. Chronic social stress induces peripheral monocyte accumulation and IL-6 passage into the NAc

A) Experimental timeline of 10-day CSDS, SI behavioral screening and tissue collection of *ccr2*^{RFP}:: *cx3cr1*^{GFP} mice. **B)** Stressed *ccr2*^{RFP}:: *cx3cr1*^{GFP} mice showed decreased SI scores following 10-day CSDS. Representative heat maps are shown on the right. **C)** Flow cytometric analysis of forebrain ccr2^{RFP+} and cx3cr1^{GFP+} cells revealed higher level of ccr2^{+} peripheral monocyte accumulation into the brain of stressed mice. Cells were gated on live CD11b^{+}F4/80^{+} (left). Numbers adjacent to gates represent percentages of ccr2^{+}cx3cr1 cells among CD11b^{+}F4/80^{+} cells. Right panel shows CD45 expression of F4/80^{+}ccr2^{+} monocytes and F4/80^{+}gfp^{+} microglia. Bar graph shows percentage of ccr2^{+}cx3cr1 cells

among forebrain CD11b^{+}F4/80+ cells. **D)** IL-6 protein level is increased in the blood and NAc of SS mice after 10-day CSDS. **E)** Dose response IL-6 i.p. injection did not change IL-6 protein level in the NAc of stress-naïve mice. **F)** Direct infusion of IL-6 into the NAc (5 min) induces social avoidance when subthreshold micro-defeat was conducted 20 min after the end of the infusion. **G)** Experimental timeline of peripheral biotinylated-IL6 injection after 10-day CSDS. IL-6-biotin-Neuravidin-Oregon 488 was detectable in the NAc parenchyma of SS mice only after 2h circulation and 5-min perfusion with PBS. **H)** Biotinylated IL-6 was also detectable in the NAc of AAV-shRNA-*cldn5*-injected mice. Data represent mean ± SEM, number of animals (*n*) is indicated on graphs. T-test for CX3CR1-GFP/CCR2-RFP mouse data, one-way ANOVA followed by Bonferroni's multiple comparison test for IL-6 protein levels and two-way ANOVA followed by Bonferroni's multiple comparison test for SI ratio after IL-6 or saline infusion, $*p < 0.05$; $**p < 0.01$; $***p < 0.001$.